Blast Loading Prediction from Peak Overpressure Data: a Case Study

Caio Barbosa Amorim[1,2], Clare Knock[2], Rene Francisco Boschi Gonçalves[1]
[1]Instituto Tecnológico de Aeronáutica (ITA), São José dos Campos/SP – Brazil
[2]Centre for Energetics Technology, Cranfield University, Defence Academy of the UK, Shrivenham SN6 8LA – United Kingdom

***Abstract* – This work assesses the performance of a methodology to predict the positive phase parameters from incident spherical free air bursts for a case study dataset of PE4 trials. The dataset comprises data within and beyond the near-field, which provides valuable insight into the near-field region. As the dataset provides no time of arrival information, the peak overpressure data will be used as the input for the methodology, which will be evaluated through the prediction error for the positive phase duration and impulse. Prediction errors increased from less than 15% beyond the near-field to more than 60% within it, indicating a substantial deterioration in prediction accuracy.**

***Keywords* – blast loading, positive phase impulse, positive phase duration.**

I. INTRODUCTION

A previous work proposed a methodology to predict incident spherical free air burst positive phase parameters for ideal explosives from time of arrival data (t_a) beyond the near-field [1]. This study aims to assess its performance for a case study of spherical PE4 charges free air bursts in the near-field and beyond it [2]. To the authors' knowledge, this is the first assessment of the proposed methodology using experimental data spanning both the near-field and beyond the near-field. This work forms part of an ongoing research project that is currently in its final stage.

As the case study does not present t_a measurements, the peak overpressure (P_{max}) and its derivative will be predicted from P_{max} measurements, which will be used to predict the positive phase duration (t_d) and impulse (I_+) for each blast wave radius (R). Fig. 1 presents a typical overpressure versus time profile caused by a blast wave and the main performance parameters associated to this.

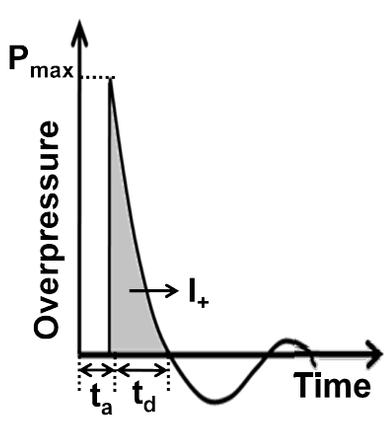

Fig. 1. Overpressure-time profile of a blast wave.

Although measured P_{max} values could be used directly, the complete methodology was intentionally followed to evaluate its performance under the same conditions for which it was originally proposed. The results will be compared to the corresponding measurements from the case study.

The literature reports a possible scattering of no more than approximately 10% for all positive phase parameters in a similar scenario of the case study of this work for TNT scaled distances (Z) from 3 to 15 m/kg$^{1/3}$ from small scale tests [3]-[4]. However, the near-field boundary is defined as the point where P_{max}/P_0 = 10 [5], where P_0 is the ambient pressure, which is equivalent to Z = 1 m/kg$^{1/3}$, approximately, according to the model from Kingery and Bulmash [6].

In the near-field, there is an additional dynamics related to the fireball influence [3]. Therefore, it is characterized by high temperature, high pressure, and is visually engulfed by the fireball. These aspects increase the difficulty for measurements acquisition from both pressure gauges and high-speed cameras. This is why there are relatively few works in the near-field region [3], so this study aims to add more insight to this less explored domain.

Additionally, the methodology under analysis is based on the assumption of an approximately constant TNT equivalence (TNTe) value [1]. Whereas the TNTe value is not expected to change for Z > 3 m/kg$^{1/3}$, it may vary within the near-field [3].

While empirical blast models, such as those based on the Kingery and Bulmash correlations [6], have been extensively used for engineering applications, most validation studies focus on scaled distances beyond the near-field [3]-[4]. Consequently, comparatively little information is available regarding the accuracy of prediction methodologies under severe near-field loading conditions, where both the blast wave characteristics and the experimental uncertainties become more pronounced. This lack of validation motivates the present assessment.

Accurate prediction of positive phase parameters in the near-field is particularly relevant for protective design because blast loading varies rapidly with distance in this region. Therefore, assessing the applicability of methodologies developed for larger scaled distances is important before they are extended to near-field engineering applications.

The performance assessment will be based on two metrics: maximum absolute deviation (MD) and mean absolute percentage error (MAPE). The desired and accepted values for each metric will be assumed as the one from the original methodology performance evaluation [1]. They will be analysed within, in the proximity of and beyond the near-field region.

C. B. Amorim, caiocba@fab.mil.br; C. Knock, c.knock@cranfield.ac.uk; R. F. B. Gonçalves, renefbg@ita.br.

II. MATERIALS AND METHODS

The case study data was acquired for R = 0.882 m, whereas the charge mass (m) varied from the detonator only, which has an explosive mass of 1.5 g, up to 1.8 kg, and all charges were initiated by the detonator only [2]. To avoid a significant influence of the detonator in the final result, only trials where the detonator does not represent more than 5% of charge mass were considered, which means m = 0.03 kg or more.

The blast parameters scaling followed a previous report proposal [7] as stated in the methodology under analysis work [1]. This procedure was intended to establish a common basis for comparative analysis of experimental data collected under different setups and environmental conditions. From now on, only the scaled parameters will be used, which will be characterized by an asterisk '*' after the variable symbol. As the test field where the trials took place is close to a sea-level altitude, and the temperature there is around 15 °C in July, when the trials occurred, no ambient pressure or temperature scaling were performed.

The case study data [2] was compiled to calculate 95% confidence interval (CI95) for all blast wave parameters in accordance with a typical statistics approach [8], and the points considered in this work with the available number of samples (NS) for each of them are presented in Table I. The relatively large number of repeated trials at each scaled distance provides a robust basis for estimating the confidence intervals used throughout the analysis.

TABLE I. BLAST WAVE PARAMETERS MEASUREMENTS COMPILATION.

R^* ($m/kg^{1/3}$)	NS	P_{max}^* (bar)	t_d^* ($ms/kg^{1/3}$)	I_+^* ($bar.ms/kg^{1/3}$)
2.83	32	1.12 ± 0.05	2.04 ± 0.07	0.75 ± 0.03
2.58	31	1.40 ± 0.06	1.81 ± 0.06	0.79 ± 0.03
2.39	32	1.58 ± 0.07	1.69 ± 0.07	0.84 ± 0.03
1.90	28	2.6 ± 0.1	1.42 ± 0.07	1.01 ± 0.04
1.32	31	6.3 ± 0.4	1.04 ± 0.08	1.3 ± 0.1
1.11	26	9.5 ± 0.5	0.90 ± 0.05	1.61 ± 0.09
0.993	29	12.8 ± 0.6	0.87 ± 0.05	1.9 ± 0.1
0.931	27	15.1 ± 0.7	1.1 ± 0.1	2.2 ± 0.1
0.882	24	16.7 ± 0.9	0.79 ± 0.08	2.0 ± 0.1
0.830	21	19 ± 1	0.74 ± 0.09	2.1 ± 0.2
0.788	19	22 ± 2	0.7 ± 0.1	2.2 ± 0.2
0.754	11	23 ± 2	0.8 ± 0.2	2.2 ± 0.2
0.725	21	24 ± 3	0.6 ± 0.1	2.4 ± 0.3

As can be seen from Table I, the data variability increases as the slant range approaches and goes further within the near-field region. This may reflect increased experimental uncertainty, measurement limitations, or physical variability associated with near-field blast propagation.

Since the proposed methodology assumes an approximately constant TNTe, verifying this assumption for the case-study dataset is an important prerequisite before evaluating the prediction accuracy. The TNTe value for each point from Table I and for the whole set will be calculated, followed by a brief analysis of its constancy along the points.

In sequence, t_d and I_+ values for each point will be predicted in accordance with the methodology under assessment [1]. This methodology is based on the shock wave theory and a hypothesis derived from it [9]-[10], and a previously published paper on P_{max} prediction [11].

Then, the predictions will be compared to the measurements with respect to the percentage difference between them, which will be used to calculate the MD and MAPE values for t_d and I_+. As discussed in a previous work, the values regarded as excellent and acceptable are, respectively, 10% and 25% for MD, and 6% and 14% for MAPE [1].

The analysis will be divided in three regions: near-field, transition, beyond near-field. These regions will be defined as $Z \leq 1$ m/kg$^{1/3}$, $1 < Z \leq 1.5$ m/kg$^{1/3}$, and $Z > 1.5$ m/kg$^{1/3}$, respectively, where Z can be calculated by Eq. (1).

$$Z = R^* / \sqrt[3]{TNTe} \quad (1)$$

III. RESULTS AND DISCUSSION

The TNTe CI95 values for each point and overall mean are presented in Table II. From Table II and the definitions from Section II, the boundaries from the near-field and the transition regions can be calculated by Eq. (1) as R* = 1.14 and 1.72 m/kg$^{1/3}$, respectively. Table II also highlights the high variability of the P_{max} measurements in the near-field, because, even with a high number of samples, the CI95 span is significant.

TABLE II. TNT EQUIVALENCE CALCULATION RESULTS.

R^* ($m/kg^{1/3}$)	TNTe
2.83	1.4 ± 0.2
2.58	1.4 ± 0.1
2.39	1.3 ± 0.1
1.90	1.3 ± 0.1
1.32	1.4 ± 0.2
1.11	1.4 ± 0.2
0.993	1.5 ± 0.2
0.931	1.6 ± 0.4
0.882	1.6 ± 0.2
0.830	1.6 ± 0.3
0.788	1.6 ± 0.2
0.754	2 ± 1
0.725	1.6 ± 0.7
Average	1.5 ± 0.2

Although TNTe variability can be high, the average TNTe (1.5 ± 0.2 as shown in Table II) overlaps by at least 50% with the CI95 of the TNTe of each individual point. This result is consistent with the hypothesis of a constant TNTe assumed by the methodology. Additionally, it indicates that changes in prediction performance are unlikely to result from significant variations in TNT equivalence. Instead, the reduction in prediction accuracy is more likely associated

with the increasing complexity of the blast wave behaviour as the near-field is approached.

Table II also shows that the confidence interval span widens as the scaled distance decreases, especially for the two lowest R* values. Since the number of samples remains relatively high for most points, this increase is unlikely to result solely from limited sampling and instead suggests greater variability in the measured blast response under near-field conditions.

The percentage differences t_d and I_+ between the predictions and measurements CI95 are presented in Fig. 2 and Fig. 3, respectively, where the vertical grid lines represent the boundaries of the near-field and transition regions.

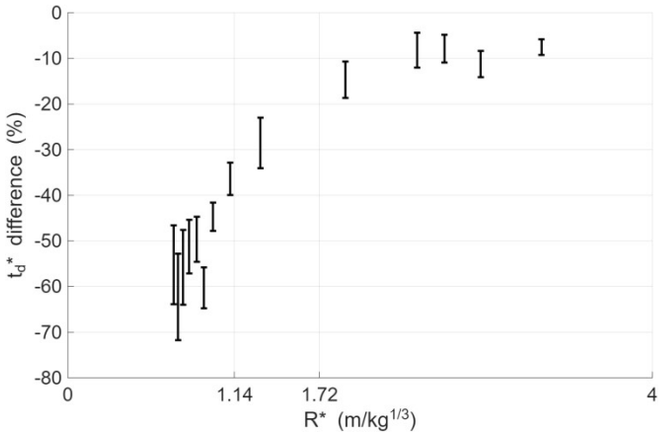

Fig. 2. Percentage difference between predictions and measurements for the t_d model.

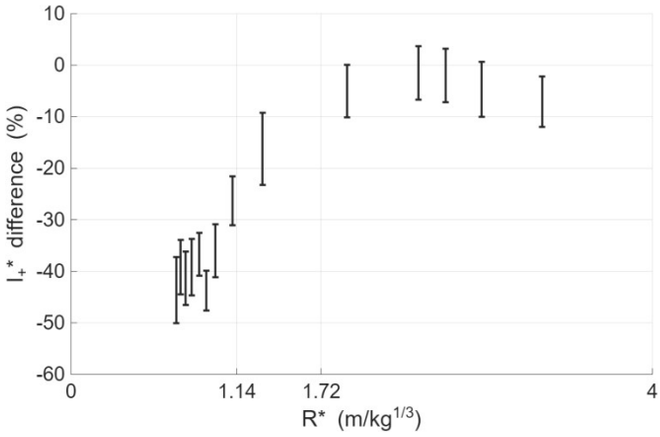

Fig. 3. Percentage difference between predictions and measurements for the I_+ model.

The MD and MAPE values for the t_d and I_+ models are shown in Table III. As there is only one point in the transition region, only MD metrics will be considered within it. Because only one experimental point lies within the transition region, statistical indicators based on multiple observations, such as MAPE, are not representative and are therefore omitted.

As can be seen from Table III, the methodology provides good results in the beyond near-field region as a previous work already verified for PE4 charges [1]. However, it provided poor results in the near-field region, and an intermediate performance in the transition region. As the blast wave radius approaches the near-field, the experimental variability increases and the prediction performance deteriorates. The transition region exhibits intermediate errors, suggesting that the degradation in prediction accuracy occurs progressively rather than abruptly at the near-field boundary.

TABLE III. MD AND MAPE VALUES FOR THE POSITIVE PHASE DURATION AND IMPULSE MODELS PER REGION

Metric		***MD (%)***	***MAPE (%)***	***Performance***
Excellent limit		10	6	Excellent
Acceptable limit		25	14	Acceptable
t_d model	Near-field	62.3	54.2	Poor
	Transition	28.5	-	Poor
	Beyond near-field	14.7	9.9	Acceptable
I_+ model	Near-field	43.8	38.5	Poor
	Transition	16.2	-	Acceptable
	Beyond near-field	7.1	4.1	Excellent

This deterioration in performance is consistent with the increased variability of the experimental data in the near-field, where nonlinear blast effects and measurement uncertainty become more significant. However, more empirical data should be analysed to verify if this is a general trend or whether it is specific to the case study dataset.

An interesting observation is that the I_+ model consistently outperforms the t_d model beyond the near-field. One possible explanation is that impulse integrates the complete positive phase and is therefore generally less sensitive to local waveform variations than t_d.

IV. CONCLUSION

This work aimed to bring further insight to the near-field behavior of a blast wave in comparison with its dynamics beyond it. For this purpose, a methodology for beyond near-field positive phase parameters prediction was applied for a dataset containing measurements within the and beyond the near-field. Data variability and prediction error were found to increase significantly as the blast wave radius approaches the near-field.

The proposed methodology maintained acceptable performance beyond the near-field but its accuracy deteriorated rapidly within the near-field. The present results also demonstrate the importance of further experimental datasets containing near-field measurements for validating blast prediction methodologies under these conditions.

From an engineering perspective, the results indicate that methodologies validated only beyond the near-field should not be extrapolated to smaller scaled distances without additional verification. This is particularly relevant for protective design applications where conservative estimates of impulse and positive phase duration are required.

The present study is limited to a single experimental dataset obtained from PE4 spherical charges free air bursts.

Although the dataset covers an unusually wide range of scaled distances, additional datasets involving different explosive types and experimental configurations would provide further confidence regarding the general applicability of the conclusions.

DATA AVAILABILITY STATEMENT

Data supporting this study are included within the article and/or supporting materials.

REFERENCES

[1] C. B. Amorim, C. Knock, D. G. Farrimond, R. F. B. Gonçalves. "A Novel Methodology for Evaluating Positive Phase Blast Wave Loading Parameters Using High Speed Video", 2026, arXiv preprint.

[2] M. D. Netherton, M. G. Stewart, S. J. Buttenshaw, K. Reidy, B. A. H. Rodgers. *Experimental Data from The University of Newcastle's July 2014 Repeatable Explosive Field Trials*. Newcastle, NSW: The University of Newcastle, 2016.

[3] D. G. Farrimond DG. "Characterisation of Blast Loading from Ideal and Non-Ideal Explosives". PhD dissertation. University of Sheffield, 2024.

[4] S. E. Rigby, A. Tyas, S. D. Fay, S. Clarke. "Validation of semi-empirical blast pressure predictions for far field explosions - is there inherent variability in blast wave parameters?", in: *Proc. 6th International Conference on Protection of Structures against Hazards*, Tianjin, China, 2014.

[5] D. L. Jones. "Blast waves and scaling laws". Phys. Fluid., vol 13, pp. 1398-1399, 1970.

[6] C. N. Kingery, G. Bulmash. *Airblast parameters from TNT spherical air burst and hemispherical surface burst*. Aberdeen Proving Ground, MD: US Army Ballistic Research Laboratory; 1984.

[7] N. C. Kingery. *Air blast parameters versus distance for hemispherical TNT surface bursts*. Aberdeen Proving Ground, MD: US Army Ballistic Research Laboratory; 1966.

[8] J. R. Taylor. *An introduction to error analysis*, 3rd ed. Sausalito: University Science Books, 1997.

[9] G. F. Kinney, K. J. Graham. *Explosive shocks in air*. 2nd ed. Berlin: Springer-Verlag; 1985.

[10] H. S. I. Sadek, J. J. Gottlieb. *Initial decay of flow properties of planar, cylindrical and spherical blast waves*. Delft, Netherlands: Delft University of Technology; 1983.

[11] C. B. Amorim, A. S. Augusto, R. F. B. Gonçalves. "A constant trinitrotoluene equivalence fit for blast wave position versus time data". Propellants Explos. Pyrotech., vol 50, pp. 44–54, 2025.